ACS OMEGA

http://pubs.acs.org/journal/acsodf
Article

Thermoplastic Polymer from Lignin: Creating an Extended Polyamide Network through Reactive Kraft Lignin Derivatives

James Sternberg* and Srikanth Pilla*

Cite This: *ACS Omega* 2023, 8, 40110−40118
Read Online

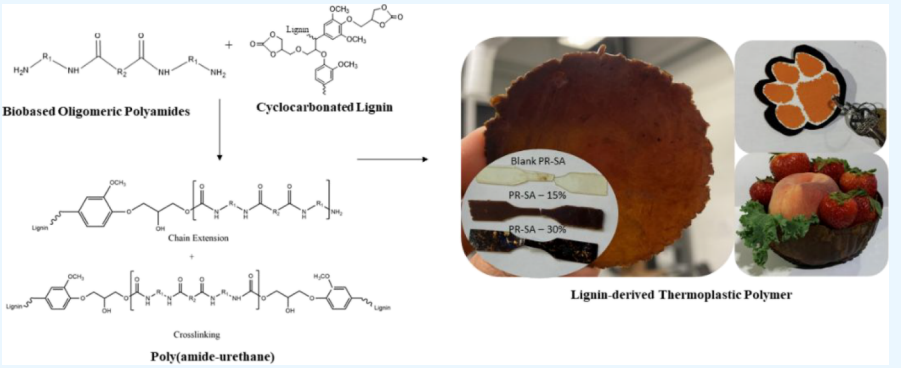

ABSTRACT: Thermoplastic polymers have many desirable properties for consumer applications and are complemented by efficient thermal processing techniques, reducing the cost of manufacturing. Lignin exists as an immense biobased carbon source but has largely been researched for its use in thermoset materials due to its own cross-linked, polyfunctional nature. In this study, a new reaction design is employed to create a thermoplastic polyamide network incorporating lignin that is tested to be 99% biobased carbon by radiocarbon analysis. Chemical analysis reveals the nature of lignin incorporation based on chain extension and cross-linking models. The thermal and rheological properties of the new polymers are thoroughly investigated to demonstrate the higher melt-strength capability of the lignin-based polymers facilitating their use in modern processing equipment. This analysis results in finding an optimal lignin loading ratio in the polymer composition reflected by improved tensile strength and stiffness. The results point to a promising polymer design for applying industrial kraft lignin in high-value thermoplastic polymer applications.

1. INTRODUCTION

Thermoplastic materials are desired for their ease of processing and recyclable nature. The plastic revolution of the last century has largely been based on low-cost, polyolefin materials that can be injection molded with rapid cycle times. The transition to biobased polymers, and in particular lignin-based polymers, entails many challenges due to the heterogeneous and cross-linked nature of the natural raw material. Lignin is an immense source of biobased carbon and composes up to 40% of hardwood and softwood trees and grasses.[1] However, its highly cross-linked structure and high concentration of phenolic and aliphatic hydroxyl groups have led to the synthesis of mainly cross-linked, thermoset materials.[2,3] In line with the biorefinery concept of the future, where natural materials substitute for petroleum-derived fuels and chemicals, many have begun to create lignin-based reprocessable materials based on thermal processing or reprocessable covalent bonds.

Efforts to mitigate the rigid structures produced from lignin and increase the processability of lignin-derived polymers have centered on incorporating long-chained molecules and oligomers in the polymeric structure based on "grafting onto" and "grafting from" approaches.[4] In the "grafting onto" approach, prepolymers and oligomers are first synthesized and then reacted with functional groups on the lignin structure. The "grafting from" approach uses lignin as the initiator of polymerization. Many groups have found the use of polycaprolactone (PCL) as a useful agent to increase the mobility of polymer chains and create a more flexible and reprocessable material. PCL can either be used as a cross-linking agent in the polymer composition[5] or used to create PCL-grafted-lignin.[6,7] Graft copolymers with polylactic acid[12] have also been created that have demonstrated thermoplastic behavior. It is also possible to create reprocessable lignin-derived polymers through the use of reversible covalent linkages. Bonding schemes based on aryl-boronate esters,[8] polybutadiene,[9] or the Diels−Alder linkage[10,11] have all been used to create lignin-based polymers

Received: April 25, 2023
Accepted: September 29, 2023
Published: October 16, 2023

https://doi.org/10.1021/acsomega.3c01259
ACS Omega 2023, 8, 40110−40118

that can be reformed from fractured materials through the use of heat and pressure. Unfortunately, in these previous reports, the concentration of lignin is often low (∼10−15%), and when the concentration is increased as with the use of polybutadiene (65−75%),[9] diisocyanates and formaldehyde are used which lowers the overall sustainability profile of the material. The overarching goal of this study was to synthesize a melt-processable, lignin-derived polymer using benign and nontoxic reagents while using 100% biobased carbon precursors to demonstrate the ability to create a high-performance thermoplastic from lignin.

Polyamides are typically produced from the condensation reaction between bifunctional carboxylic acids or acyl halides and nucleophilic diamines that require precise reaction stoichiometry to reach large molecular weights.[13] As technical lignin from biomass falls outside of this structural category, no reports for a lignin-based polyamide currently exist, only those for model compounds that can be produced from lignin.[3] The challenge of synthesizing a lignin-derived polyamide is heightened by the high melting temperatures of commercial polyamides such as PA6,6 (T_m ∼ 270 °C) and PA6,10 (T_m ∼ 220 °C) that exist above the thermal stability of lignin. However, using long-chained fatty acid−based monomers in the synthesis of the oligomeric polyamides (OPAs) can reduce the melting point of the precursors below 100 °C and render them capable of reacting with lignin to create an extended polyamide network based either on chain extension or cross-linking models. Poussard et al.[14] have synthesized amine-terminated oligomeric polyamides capable of curing cyclocarbonated precursors toward the formation of a nonisocyanate poly(urethane-amide). Dicarboxylic acids are reacted with a slight excess of diamines to create the long-chained oligomer. Initially, carbonated soybean oil was used to create urethane networks although a subsequent study extended the technology to cyclcarbonated PEG capable of foaming with supercritical CO_2.[15] The successful reaction of the oligomeric diamines with cyclocarbonates opens the door to envision other cyclocarbonated systems, such as lignin. In addition, the thermoplastic nature of polyamides creates a unique opportunity to enable a new lignin-based melt-processable system.

This study reports the synthesis of new oligomeric polyamides (OPAs) from the combination of fatty acid−based diamines, traditional diamines, and carboxylic acids of different chain lengths to react with cyclocarbonated lignin and synthesize a new polymer structure. The new polymers contain between 15 and 65% lignin and demonstrate increased mechanical properties and thermoplastic behavior. The cured materials are submitted to an extensive rheological analysis that compares the novel materials to both virgin OPAs without lignin and commercial polyamides, showing the new polymers to have increased melt strength to facilitate modern thermal processing techniques. The results reveal the ability of cyclocarbonated lignin (CC lignin) to react with the OPA precursors and increase the rheological and mechanical properties of the material while creating a polymer with 99% biobased carbon without the use of harmful and toxic reagents.

2. EXPERIMENTAL SECTION

2.1. Materials. Kraft lignin for this study was supplied by Domtar under the trade name "BioChoice Lignin". Biochoice is a low-ash-content lignin (∼1%) and was dried before use. The curing agent was kindly provided by Croda under the trade name "Priamine 1074". Priamine is a dimer diamine manufactured from natural fatty acids with an amine value of 209 mg KOH/g. Glycerol carbonate (DMC) was purchased from Spectrum Chemical or InKemia Green Chemicals with a minimum purity of 90%. Adipic acid (>99%), Dimethyl carbonate (>99.0%), dimethyl sulfoxide-d6 (DMSO-d6, 99.96 atom % D), 1,5,7-triazabicyclo[4.40]dec-5-ene (TBD, 98%), polyamide 6,6, polyamide 6,12 and poly(methylhydrosiloxane) (PMHS) was purchased from Millipore Sigma. DMSO (99%) was purchased from VWR. ACS-grade dioxane was purchased from Macron.

2.2. Synthetic Techniques. *2.2.1. Synthesis of Cyclocarboanted Lignin.* Cyclocarbonate groups were inserted on the lignin backbone according to a previous report.[16] Briefly, lignin was oxyalkylated with glycerol carbonate at 150 °C for 1.5 h. After precipitation, washing, and drying, the product was used in a transesterification reaction with dimethyl carbonate at 75 °C for 4 h to produce cycolocarbonate groups in a concentration of 2.1 mmol/g lignin.

2.2.2. Synthesis of Oligomeric Polyamide. Oligomeric polyamides (OPA) were synthesized in a nitrogen environment by loading the diamine and dicarboxylic acid without solvent in a molar ratio of 1.2:1 to produce amine terminated chains. The diamine (Priamine 1074 or hexamethylene diamine) and carboxylic acid (sebacic or adipic acid) were loaded in a round-bottom flask and allowed to reach dissolution at 160 °C. The temperature was then increased to 190 °C, and the reaction was allowed to continue for 3 h. No vacuum was applied to remove the small amount of water produced, as the goal was to produce low molecular weight oligomers rather than high molecular weight polymers. When the reaction was complete, the molten product was poured into a silicon mold and allowed to cool to room temperature.

2.2.3. Synthesis of Lignin-Derived Poly(amide-urethane). In a 10 mL beaker, the OPA was heated to its melting point. Cyclocarbonated lignin (CL) was first dissolved in DMSO and heated to the same temperature as the OPA and then added to the beaker. The percent lignin was varied based on the total mass of OPA and lignin. The two components were allowed to stir for 2−3 min and then poured into an aluminum or silicon mold and allowed to cure in an oven at 120−150 °C for 12 h. If the solvent had not been completely removed from the system after 12 h, additional heating under vacuum was used to dry the sample.

2.3. Characterization. *2.3.1. Chemical Analysis.* Infrared spectra were collected by a Thermo 6700 spectrometer from 500−4500 cm^{-1} using 16 scans with a 2 cm^{-1} spectral resolution.

2.3.1.1. Amine Value of the Oligomeric Polyamide. OPA was then dissolved in a solvent mixture of 1:1 hot toluene and isopropyl alcohol. The amine value was determined by titrating with a standardized solution of 1 M HCl in isopropyl alcohol using bromocresol green as an indicator. The endpoint was determined when the dark blue solution reached a green color. Three titrations were averaged for accuracy.

2.3.1.2. Soxhlet Extraction. Extraction was completed using a porous thimble to contain the polymeric material and allowed to cycle for 24 h. The residence time of the solvent in the trap was ∼23 min allowing for approximately 60 cycles of extraction. Poly(amide-urethanes) were extracted using a 1:1 mixture of toluene and isopropyl alcohol and found to be efficient at dissolving the OPA. When extraction was completed for both materials, the polymer was removed and allowed to dry under vacuum and weighed the following day to calculate the mass change. The percentage of residual material was calculated according to the following equation:

https://doi.org/10.1021/acsomega.3c01259
ACS Omega 2023, 8, 40110−40118

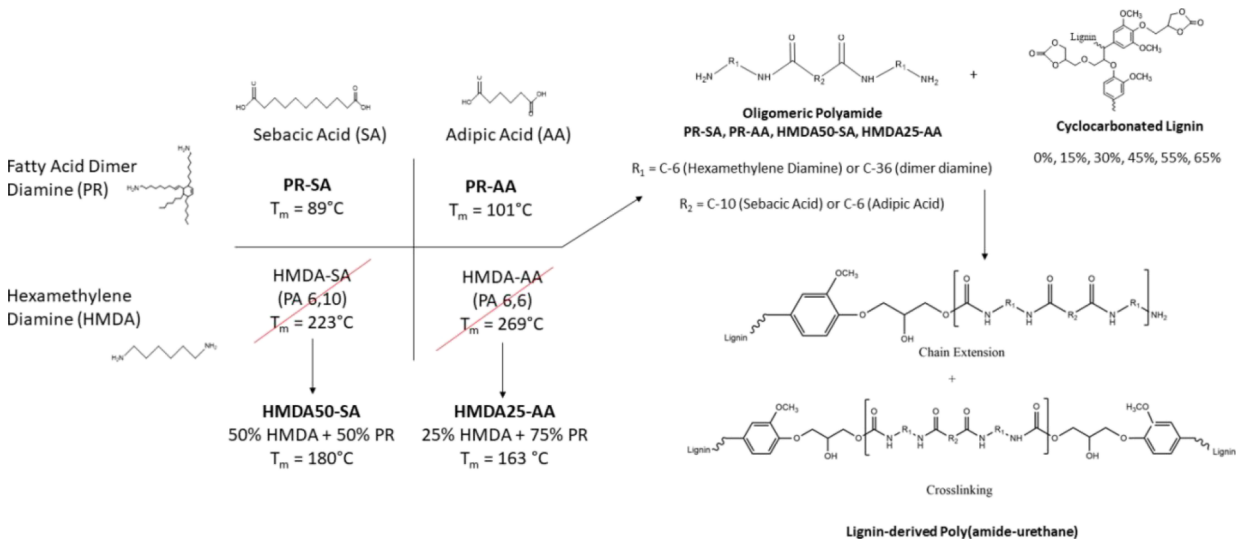

Figure 1. Outline of the different oligomeric polyamides synthesized in this study and their use to create new lignin-derived poly(amide-urethanes) with the addition of cyclocarbonated lignin.

$$X = \left[\frac{m_e}{m_i}\right] \times 100$$

where X is the residual percentage, m_i is the initial mass of the polymer, and m_e is the mass after extraction. Three runs for each polymer were used to determine the average and standard deviation.

2.3.1.3. Water Adsorption. Water adsorption of traditional and lab-synthesized polyamides was tested according to ASTM D570 using 24 h water immersion with some modifications to sample size. Samples were processed in rectangular molds of approximately 2 cm × 1 cm × 3 mm and dried overnight under vacuum at 40 °C to prohibit oxidation or degradation. Next, samples were allowed to soak for 24 h in water purified by reverse osmosis. After completion of the test, samples were spotted dry with a cloth and immediately weighed. The percent water adsorption was calculated based on the increase of mass after water immersion.

2.3.2. Thermal and Mechanical Analysis. Tensile testing of NIPU materials was completed on dog bone-shaped samples formed either from punching samples from a compression molded film or through curing in a silicon mold with a narrow section of 25 mm length, 2.5 mm width, and 2.5 mm depth according to ASTM D638. Compression molding was completed at 110 °C and 25 MPa for 10 min. Samples were tested on an Instron 1125R instrument with a 1 kN load cell at 5 mm/min. The modulus was calculated for both tensile and compression samples based on the linear region of the stress−strain curve.

Rheological analysis of the samples was completed on a TA Instruments Discovery HR-2 rheometer. Isothermal strain sweeps were completed at 110 °C for samples composed of Pr-SA and Pr-AA while samples composed of Pr50-HMDA50-SA and Pr75-HMDA25-AA were completed at 210 °C to ensure the molten state of the polymer. Sweeps from 1 to 100% strain were completed to determine the linear viscoelastic region (LVR), yield point (γ_y), and flow point (γ_f) samples. The γ_y was taken at the onset of the decrease of the storage modulus (E') while γ_f was taken at the crossover point of E' and E''. Isothermal frequency sweeps were completed at strain values determined from the LVR and conducted at the same temperature for the respective samples as the strain sweep. A frequency range of 0.1−100 rad/s was used to evaluate E', E'', and complex viscosity. Curing rheology of poly(amide-urethanes) was completed at 120 C, 1% strain, and an angular frequency of 10 rad/s.

Dynamic scanning calorimetry was completed on a TA Instruments Q20 during a heat−cool−heat cycle at 10 °C/min with 50 mm/min nitrogen purge.

3. RESULTS AND DISCUSSION

3.1. Synthetic Design. The goal of this study was to synthesize a 100% biobased lignin-derived thermoplastic through the combination of low melting point amine-terminated OPAs and cyclocarbonated lignin, creating a poly(amide-urethane). First, low T_m OPAs were synthesized from a slight excess of fatty acid−based diamine and either biobased sebacic (C-10) or adipic (C-6) acid. From these two relatively low T_m precursors (~90−100 °C), a second set of higher melting point oligomers have been synthesized by mixing different feed ratios of hexamethylene diamine (HMDA) and the fatty

acid−based dimer diamine with adipic or sebacic acid to create PA6,6 and PA6,10 analogs with melting points below 190 °C. The design for the synthesis of the 4 different OPAs is described in Figure 1. One point of emphasis with the higher melting point oligomers is the 190 °C threshold based on the boiling point of the solvent (DMSO) used to ensure a homogeneous mixture between CC lignin and the OPA. After the synthesis of the OPAs, CC lignin is added from 15 to 65% with the aid of DMSO, and these materials are cured for 12 h between 120 and 150 °C. The reaction is made possible by the attack of amine groups of the OPA on the CC groups on lignin. The reaction scheme for the synthesis of the lignin-based poly(amide-urethane) is also presented in Figure 1.

The success of the OPA synthesis was verified by FTIR monitoring the disappearance of the carboxylic carbonyl group at 1715 cm^{-1} and the appearance of the amide band at 1650 cm^{-1} as well as the secondary amine stretch at 3300 cm^{-1} (Figure S1). The spectra for all of the OPAs showed very similar characteristics using FTIR. The concentration of amine-terminated species present in the OPA was measured for the soluble samples (PR-SA, PR-AA) through an amine titration.

https://doi.org/10.1021/acsomega.3c01259
ACS Omega 2023, 8, 40110−40118

The addition of HMDA to form HMDA50-SA and HMDA25-AA resulted in insoluble materials due to the high chemical resistivity of typical polyamides. Table 1 shows that the amine values for PR-SA and PR-AA were similar to each other and agree well with the value obtained by Grignard et al.[15] (0.236 mmol/g) through the use of 1,2-diaminoethane as the amine component.

Table 1. Characteristics of the Precursors Used To Synthesize the Lignin-Derived Poly(amide-urethane)

OPA	amine value (mmol/g)	M_w	M_n	T_m (°C)
PR-SA	0.235	3200	1200	92
PR-AA	0.272	3600	2900	101
lignin	CC groups (mmol/g)	M_w	T_g (°C)	CC groups/lignin
CC-lignin	2.1	14,000	151	28

Table 1 also displays the molecular weight of the OPAs determined by gel permeation chromatography. A molecular weight of around 3500 corresponds to a degree of polymerization between diamine and diacid around 4. These molecular weights are much lower than those of typical polyamides, which reach into the 20−30 kDa region. The low molecular weights presented here are part of the reaction design to increase the number of chain-terminated amine groups capable of reacting with CC lignin. DSC (Figure S2) confirmed the ability to create low melting temperature precursors with the use of the fatty acid diamine. On the other hand, when HMDA was used as an amine component, much higher melting points for the resulting OPA's were achieved (163−180 °C, Figure S3, S4).

3.2. Chemical Analysis. The reaction of CC lignin and OPA was monitored by using FTIR by following the conversion of the cyclocarbonate peak observed at 1795 cm^{-1} to that of the urethane carbonyl at ∼1720 cm^{-1}. The reaction of PR-SA and CC lignin was chosen as the model formulation to study this reactivity. The presence of the urethane signal is an important parameter witnessing the formation of a new chemical structure present in the polymer as opposed to the formation of a polyamide blend with lignin. Figure 2A shows the evolution of the urethane peak as the concentration of lignin increases from 15 to 45%. The presence of both CC groups and urethane signals corresponds to the reaction stoichiometry present between the CC lignin and amine. Given a CC content of 2.1 mmol/g and molecular weight of 14,000,[16] each formula unit of lignin contains approximately 28 CC groups. Given the amine value of ∼0.235 mol/kg, it is expected that some of these groups will undergo a reaction and others will not. However, as Table S1 shows, the ratio between amine and CC never exceeds 28:1, the point at which lignin would begin acting as a filler rather than incorporated into the polymer structure. The increase in lignin percentage also gives rise to the characteristic peaks associated with the lignin aromatic backbone shown at 1500 and 1270 cm^{-1} and a decrease in the amide peak associated with the OPA present at 1650 cm^{-1}. The broad nature of the urethane peak is a sign of the different chemical environments of the urethane bond as well as the different hydrogen bonding interactions resulting from the new hydroxyl group formed in the ring-opening reaction of the CC group. FTIR supports the reactivity between the OPA and CC lignin, confirming the presence of a new chemical structure in the creation of a lignin-derived poly(amide-urethane). Similar FTIR spectra were obtained for the reaction of the CC lignin with the high melting point OPAs (HMDA50-SA and HMDA25-AA) revealing a similar evolution of the urethane peak (Figure S5).

The reactivity between CC lignin and the amine-terminated OPA was further characterized by monitoring the curing reaction at a 30% lignin concentration through rheology. The gel point of the reaction was determined by finding the crossover point between the storage and loss modulus on a parallel plate rheometer at 120 °C. In addition, a control experiment was carried out using raw kraft lignin that did not contain CC groups with the OPA. The control experiment represents a material where lignin is physically blended with the OPA, however, given the various chemical groups present in lignin as well as the propensity of lignin to undergo molecular arrangements at elevated temperatures, cross-linking is still expected to occur. The reaction between CC lignin and PR-SA reaches a gel point at 42 min and the storage modulus reaches above 10^{-2} MPa after

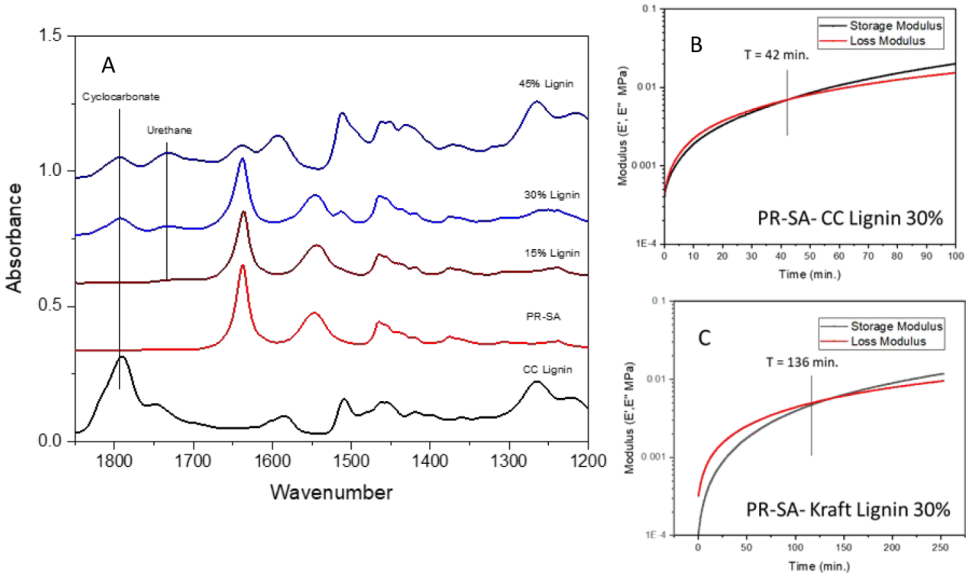

Figure 2. FTIR of PR-SA and 0−45% lignin (A) and curing rheology of the reaction mixture of PR-SA and 30% lignin (B) and a control study using raw kraft lignin (C).

https://doi.org/10.1021/acsomega.3c01259
ACS Omega 2023, 8, 40110−40118

just 100 min (Figure 2B). Conversely, the control reaction with PR-SA and unmodified Kraft lignin reaches a gel point after 136 min and reaches a storage modulus of 10^{-2} MPa after 250 min (Figure 2C). The gel time of the control reaction is more than 3 times longer than the reaction with CC lignin, pointing to the reaction of CC groups and amines. An even more dramatic result is observed for the reaction mixture containing PR-AA where a gel point was determined at about 10 min (Figure S6). The faster gel time observed for PR-AA is most likely due to the higher amine value associated with this OPA (Table 1). The rheological experiments complement the findings from FTIR that CC lignin and the amine-terminated OPA successfully react, creating new chemical linkages in the form of urethane bonds. This new chemical structure results in significant changes to the viscoelastic behavior of the polymer, as will be seen below.

Soxhlet extraction of the cured material was completed using a solvent efficient at dissolving the neat OPA. Residual material reflects the degree of reaction between OPA and lignin, given that the lignin precursor did not dissolve in the 1:1 isopropanol/toluene mixture used in the analysis. The results showed an increase in the residual amount with increasing lignin concentration. At 15% lignin concentration, an average of 26.0% residual material was recovered, whereas at 30 and 45% lignin this amount increased to 60.6 and 64.4% respectively. The increased residual amount at 30% lignin is a result of the higher concentration of CC groups creating urethane bonds with the OPA. The presence of both extracted and residual material reflects the existence of a phase-separated material composed of neat OPA and that of chain-extended and/or cross-linked OPA with CC lignin. However, the ability to melt-process the material was confirmed by rheological studies (see below) demonstrating the final polymer was not fully cross-linked. An initial indication of an optimal concentration of CC lignin is demonstrated by the small increase of residual material at 45% lignin, representing a significant amount of lignin as filler beyond the 30% concentration level. Additional analysis was completed on samples composed of PRSA and 30% lignin showing low water adsorption ($1.62 \pm 0.23\%$, Table S2) and 99% biobased content based on radiocarbon analysis (ASTM 6866, see discussion in SI), further confirmation of an optimized lignin loading ratio.

3.3. Thermal Analysis. The melting points and heat of fusion values (ΔH_f (J/g)) of cured resins were gained from the second heating cycle of DSC analysis and are organized in Table 2. The general trend is observed that increasing lignin concentration results in a decrease in the melting point as well as a decrease in the crystallinity (smaller ΔH_f values) compared to the neat OPA. Only samples resulting from low T_m OPAs have measured ΔH_f values due to the multiple endotherms present in the high T_m OPAs. The two results are complementary: as the lignin content increases and disrupts the orderly arrangement of the OPA, the melting point is lowered as well as the overall crystallinity of the sample. In addition, the reaction with lignin creates amorphous phases that do not have a distinct T_m and further decrease the ΔH_f. Similar results were found by Oh et al. in their study of adding diamine chain extenders to PA6.[17] In their study, the chain extender was added in much lower proportions (~0.1−0.2 mol % based on PA6 reactive groups) creating a material with lowered crystallinity.

Table 2. Melting Points and Heat of Fusion for Polymer Formulations Used in This Study

lignin (%)	PR-SAT$_m$ (°C)/ΔH_f (J/g)	PR-AAT$_m$ (°C)/ΔH_f (J/g)	HMDA50-SAT$_m$ (°C)	HMDA25-AAT$_m$ (°C)
0	92.1/15.4	100.4/10.6	177.0	162.9
15	89.7/15.6	89.8/7.7	168.3	148.8
30	85.8/10.8	85.5/4.4	169.6	157.0
45	85.2/4.5	86.6/5.0	154.2	143.7

The DSC results presented here are important to the objective of creating a lignin-derived thermoplastic. The preservation of a melting point, albeit with lowered crystallinity, represents the thermoplastic character of the lignin-derived poly(amide-urethane). The goal of synthesizing a lignin-derived thermoplastic stems from the desire to combine the environmental benefits of using biobased precursors with manufacturing benefits gained with a melt-processable material. The thermoplastic nature of the materials enables their use in modern industrial processing techniques such as extrusion, thermoforming, and injection molding.

3.4. Rheological Analysis. Rheological experiments of cured materials were carried out to explore the thermomechanical properties of polymers containing different compositions of lignin. Strain sweeps were conducted at 10 rad/s from 0.1% to 100% strain to evaluate the extent of the linear viscoelastic region in each polymer composition. Table S3 displays the yield and flow points of each polymer composition used in this study. Corresponding graphs for each polymer can be found in Figures S7, S8. The general trend is observed that increasing lignin content results in a faster onset of the yield and flow point (i.e., at lower strain values) due to the rigid nature of lignin. The curves for all strain sweeps represent smooth transitions to the flow point except for polymers composed of HMDA. The shorter chain length of these monomers imparts a higher degree of hard segments, resulting in the brittle behavior of the polymer.

For all polymer compositions, a relatively large increase in the storage modulus is observed between samples with 15 and 30% lignin. From 30 to 45% lignin, a smaller increase is observed. Given the extended LVR associated with samples composing 30% lignin (Figure S7), the strain sweep experiments confirmed the identification of the lignin composition, resulting in polymers with enhanced properties. The LVR associated with 30% lignin also sheds light on the nature of the polymer matrix. The preservation of the LVR reveals that the new polymer is not dominated by a cross-linking motif with lignin but rather maintains the ability to undergo increasing softening that is associated with amorphous polymers. At 45% concentration, lignin may begin to take on filler effects imparting excessively brittle characteristics to the polymer network, as witnessed by the faster onset of the yield and flow point (Table S3).

Frequency sweeps of the cured polymers were completed at ω = 0.1−100 rad/s using a strain value from the linear viscoelastic region determined for each polymer. Starting with polymers composed of PR-SA, the neat OPA displays typical liquid behavior with E'' above E' (Figure 3). According to linear viscoelastic behavior, E' should show proportionality to ω^2 (angular frequency) while E'' should vary as ω.[17] The result of this relationship is the separation of E' and E'' by at least an order of magnitude for linear polymers following a typical LVR. While the neat polyamide obeys this relationship, the reaction with CC lignin creates a new structure where this proportionality to ω is lost. The reaction with 15% CC lignin increases the value of the storage modulus by 4 orders of magnitude, while an increase of 1 order of magnitude is observed between 15 and 30% lignin and smaller increases at higher lignin concentration.

https://doi.org/10.1021/acsomega.3c01259
ACS Omega 2023, 8, 40110−40118

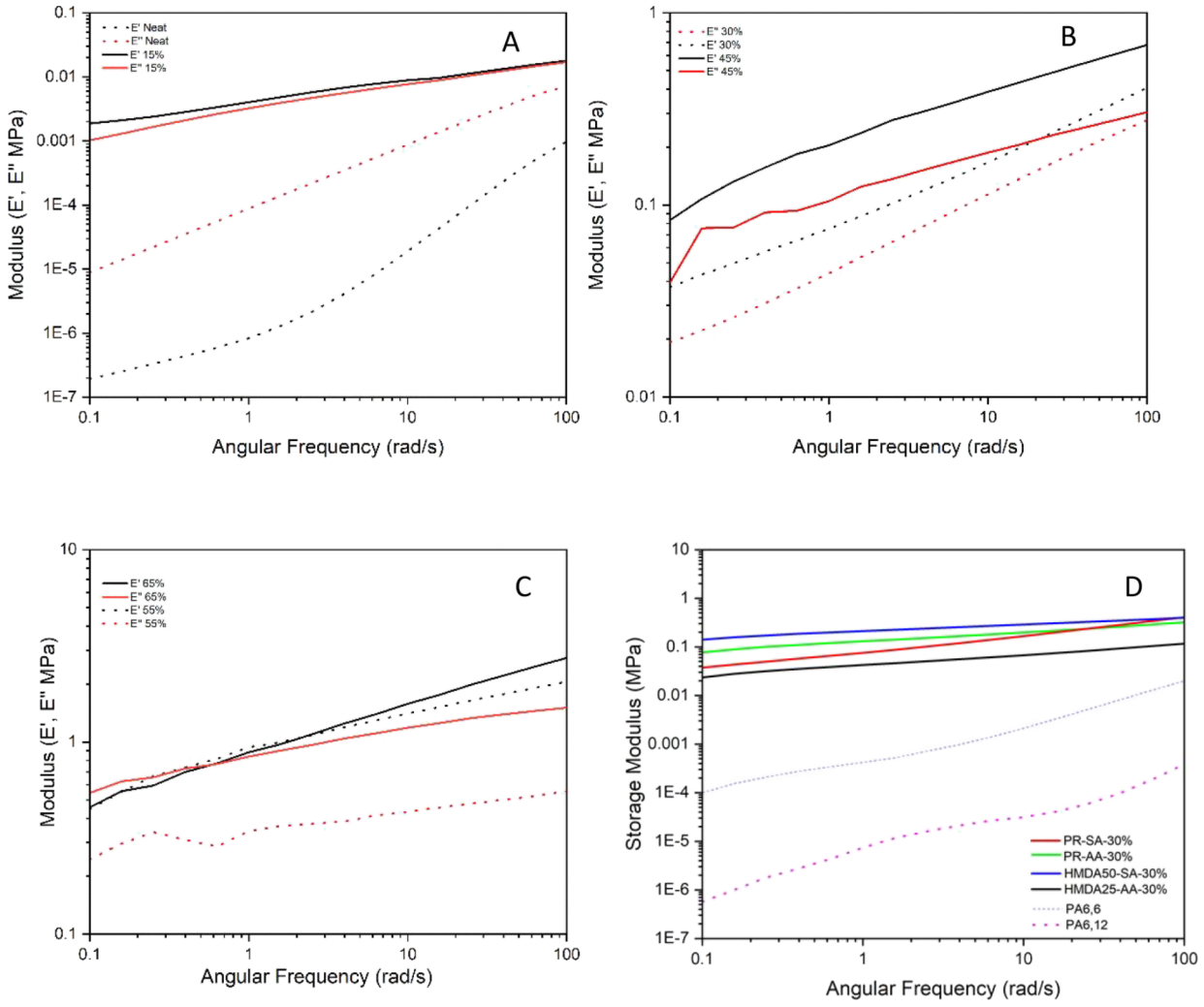

Figure 3. Rheological frequency sweeps of poly(amide-urethanes) composed of PR-SA and 0−65% lignin (A−C) and *E′ at 30% lignin concentration for all polymer compositions compared to commercial polyamides (D).*

Frequency sweeps for polymer compositions containing other OPAs are found in Figure S9 and follow the same trends observed for PR-SA. In order to compare all polymer systems, Figure 3D displays E' for 30% lignin composition in each OPA. Consistent behavior is observed based on the hard segment composition of the OPA and the magnitude of E'. These results point to the importance of neat OPA and the influence that it has on the final network structure of the cured resins. As with linear thermoplastic polymers, single-phase, crystalline materials tend to result in higher mechanical properties.[17] The storage modulus at 30% lignin composition is also compared to that of traditional PA6 and PA6,12 in Figure 3D. The new polymer structure afforded by the reaction of OPAs with CC creates a much higher modulus in the melt state compared to traditional polyamides. These modulus values correspond to one of the objectives of this study, namely, creating a high-melt-strength material facilitating traditional thermal techniques such as extrusion and injection molding.[17−20]

The complex viscosity of the cured material is tied to the changes in E' and E''. Low melting point OPA's (PR-SA, PR-AA) contain a broad Newtonian plateau, as neat polymers seen by the constant viscosity in the frequency range tested (Figure 4A). Newtonian behavior is consistent with linear polymers in a narrow molecular weight distribution.[20] However, HMDA50-SA (a high T_m of the OPA) displayed a non-Newtonian curve through shear thinning behavior with increasing angular frequency. Shear thinning is a result of large molecular weight distributions present in the polymer sample.[20] Only HMDA50-SA is given in Figure 4 due to inconsistent results observed for HMDA25-AA. For linear polymers, the viscosity generally follows the 3.4 power law ($\eta \sim M^{3.4}$) where η is the viscosity and M is the molecular weight.[17] Although lignin is not a linear molecule, even a weak correspondence to the power law could reveal structural details about the polymer structure between 15 and 30% loadings. Table S4 shows the values for complex viscosity calculated for chain extension, assuming one OPA reacts with one CC lignin molecule. The result shows that at 15% lignin content, the observed complex viscosity corresponds to the same order of magnitude as the viscosity calculated through the power law. This relationship breaks down at 30% lignin, where the observed value is more than an order of magnitude higher than that calculated for chain extension. Given these results, it is most likely that chain extension is the dominant structure at 15% lignin loading whereas at 30% cross-linking branching becomes more prevalent. This behavior is only consistent with polymers composed of the low T_m OPAs as HMDA50-SA has very similar η^* values for both 15 and 30% lignin loadings (Figure 4C).

https://doi.org/10.1021/acsomega.3c01259
ACS Omega 2023, 8, 40110−40118

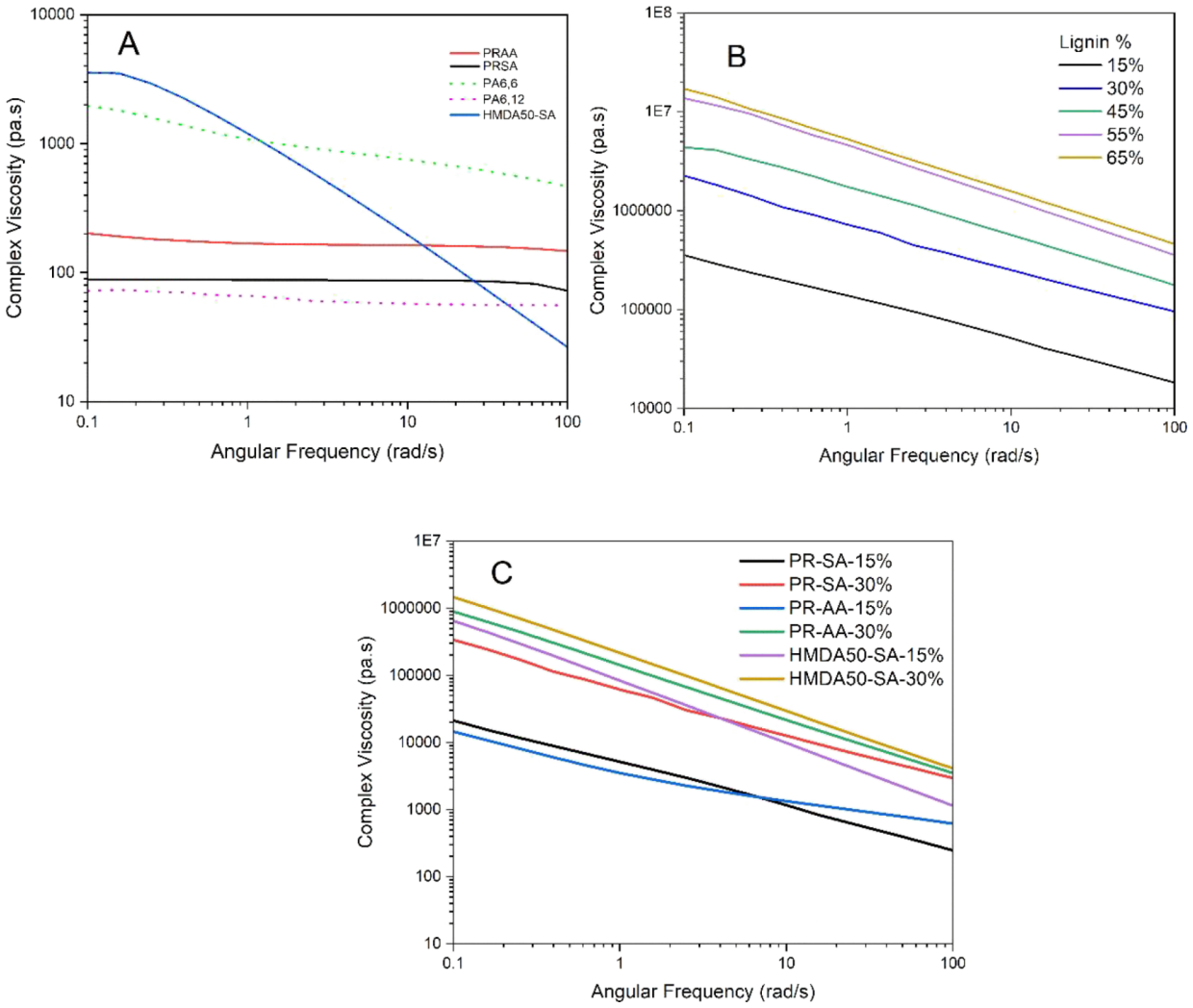

Figure 4. Complex viscosity for (A) neat OPAs compared to PA6,6 and PA6,12; (B) increasing lignin content from 15−65% with PR-SA; (C) comparison of 15 and 30% lignin contents for high and low T_m OPAs.

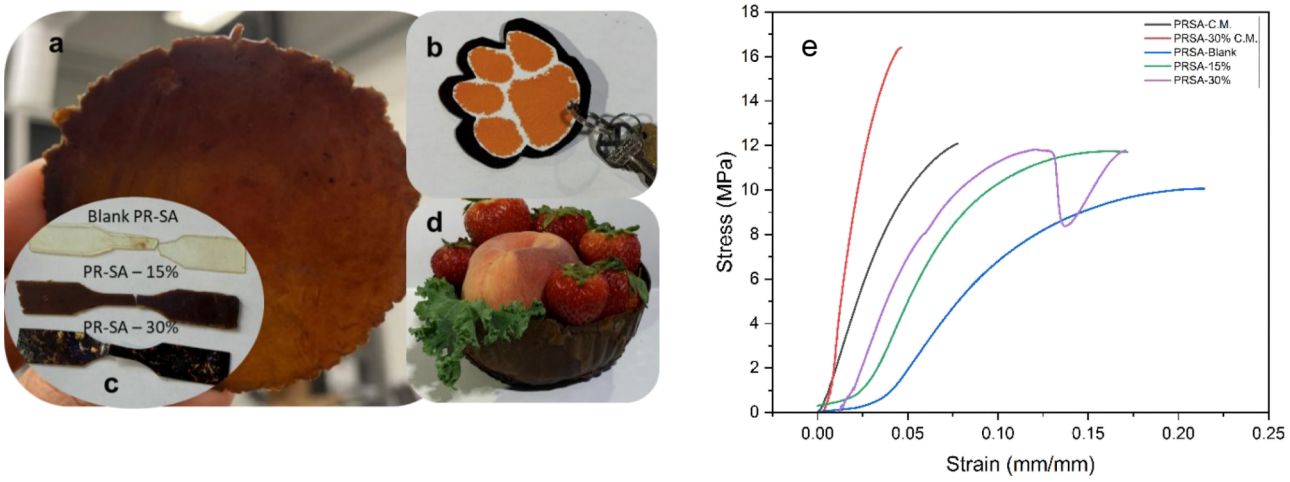

Figure 5. Demonstration of the thermoplastic character of PRSA-15%: (a) the ability to form sheets, (b) the ability to cut into various shapes, (c) the ability to create dog-bone samples, (d) the ability to thermoform into a simple bowl, and (e) stress−strain graph dog-bone style test samples.

The complex viscosities of PA6,6 and PA6,12 are also represented in Figure 4A showing surprising correspondence to the neat low T_m OPAs (c.f. PR-SA, PR-AA with PA6,12) and to the high T_m of the OPA HMDA50-SA (c.f. PA6,6). The design of these OPAs was in fact to mimic traditional polyamides yet with processing temperatures that enable reactions with CC lignin. After reaction with CC lignin, the new poly(amide-urethanes) exhibit 3−4 orders of magnitude higher η^* than

https://doi.org/10.1021/acsomega.3c01259
ACS Omega 2023, 8, 40110−40118

PA6,6 and PA6,12 creating new materials with enhanced processing characteristics.

These new polymers with enhanced melt viscosity address the problems associated with low bead strength typically encountered with highly used commodity polyamides.

3.5. Mechanical Properties. Tensile testing of dog-bone-shaped samples was completed to understand the structural effect of cross-linking with increasing lignin content (Figure 5e and Table 3). The neat polyamide chosen for analysis was PRSA consistent with the emphasis placed on this formulation in our study. The results show that very similar mechanical properties are recorded for the blank sample and those with 15% lignin. The addition of 15% lignin disrupts the natural crystallinity of the polyamide but also increases the chain length of the polyamide, leading to a net balance of mechanical properties. However, at 30% lignin, an increase in ultimate tensile strength and modulus is observed as a result of the increased cross-linking demonstrated by these samples. Due to some heterogeneous properties observed at 30% lignin, compression molded (C.M.) samples were created to reduce the effect of voids that could be present in the samples cured at atmospheric pressure. The images of the compression molded sample of 30% lignin (Figure 5c) also reveal some separation of lignin-bound phases from neat OPA. While the tensile strength of the samples at 30% lignin was increased slightly, the modulus saw an over 2-fold increase in stiffness. This was also consistent with the blank samples to a somewhat smaller degree. This increase in properties over the samples cured at atmospheric pressure reflects the tighter packing of the polymer matrix under the 25 MPa pressure used for compression molding. These data confirm the structural analysis given earlier, namely, that the incorporation of lignin at the 30% level increases the mechanical properties through cross-linking while maintaining the ability of the polymer to be melt-processed. Figure 5 also displays the ability of the lignin-based polyamide (PRSA-15%) to be flattened into sheets (Figure 5a), cut into shapes (Figure 5b), and thermoformed into a bowl-like structure for packaging applications (Figure 5d). These simple demonstrations validate the thermoplastic character of the new polymer, despite the reaction with the multifunctional character of lignin.

Table 3. Tensile Testing Results of PRSA at 0, 15, and 30% Concentration with C.M. Representing Compression Molded Samples

sample	ultimate tensile strength (MPa)	strain at break (% elongation)	modulus (MPa)
PRSA-blank	11.2 ± 1.0	33.8 ± 26.3	130.4 ± 30.1
PRSA-C.M.	12.4 ± 0.3	7.9 ± 1.1	262.1 ± 31.0
PRSA-15%	11.3 ± 0.6	26.7 ± 7.6	147.3 ± 16.2
PRSA-30%	13.2 ± 1.2	18.3 ± 10.1	184.4 ± 22.3
PRSA-30% C.M.	15.0 ± 1.5	6.1 ± 1.4	453.8 ± 83.0

4. CONCLUSIONS

The new poly(amide-urethanes) synthesized in this report achieve the goal of creating a thermoplastic polymer from industrial kraft lignin while increasing the processing capability of the polymer in the melt state. While the melt temperature of the materials using the fatty acid–based diamine is much lower than typical polyamides, this enables lignin to participate in the polymer structure and produce polymers with low water adsorption, increased mechanical properties, and 99% biobased carbon content. This study aimed to find a high-volume and high-value use for industrial kraft lignin; in this sense, the ability to change the lignin content and transition from chain extension to cross-linking models is significant. At lower lignin content (15%) the properties resemble chain extended polyamides with a 3 orders of magnitude increase in the complex viscosity and storage modulus of molten samples. At higher lignin concentrations (30%) further stiffening of the polymer matrix occurs, providing the opportunity for an increase in tensile strength and modulus. These new materials not only address the need for thermoplastic materials from lignin but also address the need for greater processability of typical polyamides. The increased viscosity and melt strength of the novel poly(amide-urethanes) can potentially overcome the difficulties with the low melt strength encountered with the high use commodity PA6,6 and PA 6,12.

The study presented here is the first of its kind to explore a lignin-derived thermoplastic based on the reaction of lignin precursors with biobased polyamides. Based on the reactivity demonstrated between CC lignin and the oligomeric polyamides as well as the preservation of the melting point of the cured materials, it is possible to envision the application of the new polymers in modern processing equipment. The inclusion of lignin in materials capable of traditional thermal processing is an important step toward the biorefinery concept, where natural materials are used as feedstocks for commercially available products. The thermoplastic character of the new polymers decreases the high-cost barrier and capital expenses often associated with thermoset polymer systems. In addition, the low water adsorption and ability to tune the final properties based on lignin content make these materials attractive for use in applications where a range of properties are needed to meet component specifications.

■ ASSOCIATED CONTENT

Supporting Information

The Supporting Information is available free of charge at https://pubs.acs.org/doi/10.1021/acsomega.3c01259.

Additional thermal, rheological, and spectroscopic data (PDF)

■ AUTHOR INFORMATION

Corresponding Authors

James Sternberg − *Department of Food, Nutrition and Packaging Science, Clemson University, Clemson, South Carolina 29634, United States;* orcid.org/0000-0003-3513-7018; Email: sternbe@clemson.edu

Srikanth Pilla − *Department of Chemical and Biomolecular Engineering, Department of Materials Science and Engineering, Department of Mechanical Engineering, and Center for Composite Materials, University of Delaware, Newark, Delaware 19716, United States;* orcid.org/0000-0003-3728-6578; Email: spilla@udel.edu

Complete contact information is available at: https://pubs.acs.org/10.1021/acsomega.3c01259

Notes

The authors declare no competing financial interest.

■ ACKNOWLEDGMENTS

This work was partially supported by the Department of Energy, Basic Energy Sciences, award no. DE-SC0021367 (thermoplastic polymer synthesis), and as part of the AIM for Composites, an Energy Frontier Research Center funded by the US Department of Energy (DOE), Office of Science, Basic Energy Sciences (BES), under award no. DE-SC0023389 (thermoplastic polymer characterization).

■ REFERENCES

(1) Ragauskas, A. J.; Beckham, G. T.; Biddy, M. J.; Chandra, R.; Chen, F.; Davis, M. F.; Davison, B. H.; Dixon, R. A.; Gilna, P.; Keller, M.; Langan, P.; Naskar, A. K.; Saddler, J. N.; Tschaplinski, T. J.; Tuskan, G. A.; Wyman, C. E. Lignin Valorization: Improving Lignin Processing in the Biorefinery. *Science* **2014**, *344*, No. 1246843, DOI: 10.1126/science.1246843.

(2) Sternberg, J.; Sequerth, O.; Pilla, S. Green Chemistry Design in Polymers Derived from Lignin: Review and Perspective. *Prog. Polym. Sci.* **2021**, *113*, No. 101344.

(3) Upton, B. M.; Kasko, A. M. Strategies for the Conversion of Lignin to High-Value Polymeric Materials: Review and Perspective. *Chem. Rev.* **2016**, *116* (4), 2275−2306.

(4) Duval, A.; Lawoko, M. A Review on Lignin-Based Polymeric, Micro- and Nano-Structured Materials. *React. Funct. Polym.* **2014**, *85*, 78−96.

(5) Zhang, Y.; Liao, J.; Fang, X.; Bai, F.; Qiao, K.; Wang, L. Renewable High-Performance Polyurethane Bioplastics Derived from Lignin−Poly(ε-Caprolactone). *ACS Sustainable Chem. Eng.* **2017**, *5* (5), 4276−4284.

(6) Hatakeyama, T.; Izuta, Y.; Hirose, S.; Hatakeyama, H. Phase Transitions of Lignin-Based Polycaprolactones and Their Polyurethane Derivatives. *Polymer* **2002**, *43* (4), 1177−1182.

(7) Jang, S.-H.; Kim, D.-H.; Park, D. H.; Kim, O. Y.; Hwang, S.-H. Construction of Sustainable Polyurethane-Based Gel-Coats Containing Poly(ε-Caprolactone)-Grafted Lignin and Their Coating Performance. *Prog. Org. Coatings* **2018**, *120*, 234−239.

(8) Korich, A. L.; Clarke, K. M.; Wallace, D.; Iovine, P. M. Chemical Modification of a Lignin Model Polymer via Arylboronate Ester Formation under Mild Reaction Conditions. *Macromolecules* **2009**, *42* (16), 5906−5908.

(9) Saito, T.; Perkins, J. H.; Jackson, D. C.; Trammel, N. E.; Hunt, M. A.; Naskar, A. K. Development of Lignin-Based Polyurethane Thermoplastics. *RSC Adv.* **2013**, *3* (44), 21832.

(10) Buono, P.; Duval, A.; Averous, L.; Habibi, Y. Thermally Healable and Remendable Lignin-Based Materials through Diels − Alder Click Polymerization. *Polymer* **2017**, *133*, 78−88.

(11) Duval, A.; Lange, H.; Lawoko, M.; Crestini, C. Reversible Crosslinking of Lignin via the Furan−Maleimide Diels−Alder Reaction. *Green Chem.* **2015**, *17* (11), 4991−5000.

(12) Han, Y.; Yuan, L.; Li, G.; Huang, L.; Qin, T.; Chu, F.; Tang, C. Renewable Polymers from Lignin via Copper-Free Thermal Click Chemistry. *Polymer* **2016**, *83*, 92−100.

(13) Kim, D. H.; Lee, J. H.; Kim, H. J. Characterization of Poly(Ether-Block-Amide)s Prepared from Oligomeric Polyamide 12 via Dispersion Polymerization. *Polymer* **2012**, *36* (4), 513−518.

(14) Poussard, L.; Mariage, J.; Grignard, B.; Detrembleur, C.; Jérôme, C.; Calberg, C.; Heinrichs, B.; De Winter, J.; Gerbaux, P.; Raquez, J.-M.; Bonnaud, L.; Dubois, P. Non-Isocyanate Polyurethanes from Carbonated Soybean Oil Using Monomeric or Oligomeric Diamines To Achieve Thermosets or Thermoplastics. *Macromolecules* **2016**, *49* (6), 2162−2171.

(15) Grignard, B.; Thomassin, J.-M.; Gennen, S.; Poussard, L.; Bonnaud, L.; Raquez, J.-M.; Dubois, P.; Tran, M.-P.; Park, C. B.; Jerome, C.; Detrembleur, C. CO_2-Blown Microcellular Non-Isocyanate Polyurethane (NIPU) Foams: From Bio- and CO_2-Sourced Monomers to Potentially Thermal Insulating Materials. *Green Chem.* **2016**, *18* (7), 2206−2215.

(16) Sternberg, J.; Pilla, S. Materials for the Biorefinery: High Bio-Content, Shape Memory Kraft Lignin-Derived Non-Isocyanate Polyurethane Foams Using a Non-Toxic Protocol. *Green Chem.* **2020**, *20*, 6922−6935.

(17) Oh, K.; Kim, H.; Seo, Y. Effect of Diamine Addition on Structural Features and Physical Properties of Polyamide 6 Synthesized by Anionic Ring-Opening Polymerization of ϵ-Caprolactam. *ACS Omega* **2019**, *4* (17), 17117−17124.

(18) Qian, Z.; Chen, X.; Xu, J.; Guo, B. Chain Extension of PA1010 by Reactive Extrusion by Diepoxide 711 and Diepoxide TDE85 as Chain Extenders. *J. Appl. Polym. Sci.* **2004**, *94* (6), 2347−2355.

(19) Dörr, D.; Kuhn, U.; Altstädt, V. Rheological Study of Gelation and Crosslinking in Chemical Modified Polyamide 12 Using a Multiwave Technique. *Polymers* **2020**, *12* (4), 855.

(20) Seo, Y. P.; Seo, Y. Effect of Molecular Structure Change on the Melt Rheological Properties of a Polyamide (Nylon 6). *ACS Omega* **2018**, *3* (12), 16549−16555.

https://doi.org/10.1021/acsomega.3c01259
ACS Omega 2023, 8, 40110−40118